

Simulating time-integrated photon counting using a zero-photon generator

Stephen C. Wein

Quandela SAS, 10 Boulevard Thomas Gobert, 91120 Palaiseau, France*

Photon counting simulations are crucial for designing and optimizing quantum photonic devices. The naive way to simulate time-integrated measurements of light requires integrating multi-variable correlations. This causes simulation times to increase exponentially with the correlation order, or number of detected photons. In this work, I present a method to simulate time-integrated quantities from the time dynamics of quantum emitters without multi-variable integration. The approach uses an effective master equation defined by a zero-photon generator—a generator of time dynamics conditioned on the absence of detected light. The zero-photon conditional dynamics depends on an efficiency parameter for each detector. These parameters can take complex values to define a set of virtual detector configurations that can be exploited to reconstruct integrated quantities using an inverse Z-transform such as a discrete Fourier transform. The method can accelerate the simulation of single-photon sources and entangled photonic resource states for measurement-based quantum computing while accounting for physical imperfections of realistic devices. It also provides a general framework to simulate interactions between stationary qubits mediated by measurements of flying qubits, which has applications to model noise for distributed quantum computing and quantum communication protocols.

Pulses of non-classical light serve as flying qubits for photonic quantum information processing [1], are important resources for quantum sensing [2], and are critical ingredients for a future quantum internet [3–5]. Combined with linear optics and photon-counting detectors, quantum states of light can be used to perform quantum computing [6–8] and quantum communication [9]. They can be generated from classical pulses using non-linear processes such as parametric down-conversion [10] or emission from single quantum emitters [11]. In particular for single emitters, the quantum dynamics of the light-matter interaction play a large role in determining the quality of the light. Capturing these dynamics is also necessary for simulating protocols that exploit emitter degrees of freedom, such as the spin of a particle, to generate entangled states of light [12] or to serve as a quantum memory [13].

Propagating pulses occupy the continuum of the electromagnetic field [14]. Hence, the physics of quantum photonic technology depends on continuous degrees of freedom, such as time or frequency, that do not need to be fully resolved when measuring the light. The naive way to simulate pulsed photon-counting experiments relies on computing field correlations in the time or frequency domain and subsequently integrating unresolved degrees of freedom to get the final measurement result. For example, simulating Hong-Ou-Mandel bunching [15] of emission from a quantum dot requires integrating the arrival time of each photon at each detector to get the total coincidence probability [16]. The consequence is that each photon-counting event contributes at least one dimension of integration, which scales poorly and generally prohibits simulating the dynamics and measurement of more than a few interacting low-energy pulses [17]. In some cases, multi-dimensional integrals can be factored into lower-dimensional integrals [18, 19], which can alleviate the scaling problem. But, this still demands a fully time-resolved simulation and it must be hand-tailored to specific scenarios.

To address this problem, I introduce a general method to simulate time-integrated quantities, such as photon-number probability distributions, without using multi-variable integra-

tion. The intuition is that it is easy to simulate the probability of measuring zero photons using perturbation theory [20–23], because there is no arrival time and hence nothing to integrate. This zero-photon probability can also be expressed as a linear combination of all higher-order probabilities weighted by powers of detector loss coefficients [24, 25]. After making this connection, I show that this loss relation extends to source conditional dynamics, multi-mode scenarios, and holds also for configurations of detectors with complex efficiencies. The result is that time-integrated quantities can be computed by applying an inverse transform, such as a discrete Fourier transform, to a set of possibly unphysical zero-photon measurements. This decreases computational cost and provides a robust numerical framework for studying a wide range of photonic experiments from boson sampling to spin-mediated cluster state generation using time-dynamic sources of light.

The method is applicable to one or more sources that evolve following a Markovian master equation defined by a linear superoperator \mathcal{L} [26] called the Lindbladian [27]. The evolution of the density operator $\hat{\rho}$ is given by $d\hat{\rho}(t)/dt = \mathcal{L}(t)\hat{\rho}(t)$ for an initial state $\hat{\rho}(t_0)$, which has the solution $\hat{\rho}(t) = \mathcal{P}(t, t_0)\hat{\rho}(t_0)$, where \mathcal{P} is the propagator $\mathcal{P}(t, t_0) = \mathcal{T} \exp[\int_{t_0}^t \mathcal{L}(t')dt']$ and \mathcal{T} orders time-dependent superoperators.

Single-mode scenario.—Suppose a source emits a pulse that is monitored by a number-resolving detector with efficiency $\eta = 1$ (see Fig. 1a). The problem is then to simulate time-integrated quantities such as the probability $p^{(n)}$ of detecting n photons in the pulse. To achieve this, one can unravel [20] the master equation using a photon-number decomposition [23]. This is done by solving the effective master equation governed by a zero-photon generator (ZPG) $\mathcal{L}^{(0)} = \mathcal{L} - \mathcal{J}$ [21], where \mathcal{J} is the linear superoperator describing the action on the source when detecting a photon, which is usually given by a Heisenberg input-output relation [28]. This ZPG is the mixed-state analog of the non-Hermitian Hamiltonian used in the quantum trajectories formalism [22].

The general solution to the effective master equation is $\mathcal{P}^{(0)}(t, t_0) = \mathcal{T} \exp[\int_{t_0}^t \mathcal{L}^{(0)}(t')dt']$, which describes the dy-

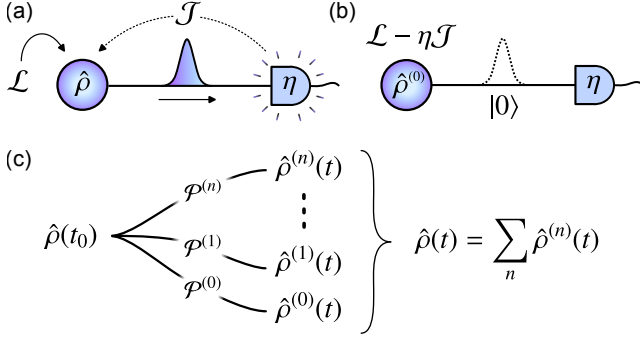


FIG. 1. **The photon-number decomposition.** (a) A source evolving with Markovian dynamics generated by the Lindbladian \mathcal{L} emits a pulse of light collected into a single mode. The pulse is measured by an ideal photon-number resolving detector with efficiency η , which induces the linear superoperator \mathcal{J} acting on the source density operator when a single photon is detected. (b) The absence of detected light conditions the source to evolve with dynamics governed by the zero-photon generator $\mathcal{L}^{(0)} = \mathcal{L} - \eta\mathcal{J}$. (c) The initial source density operator $\hat{\rho}(t_0)$ is decomposed into states $\hat{\rho}^{(n)}(t) = \mathcal{P}^{(n)}(t, t_0)\hat{\rho}(t_0)$ conditioned detecting n photons between time t_0 and time t , where $p^{(n)} = \text{Tr}[\hat{\rho}^{(n)}]$ is the probability of detecting n photons.

namics of the source conditioned on detecting zero photons (see Fig. 1b). The full propagator \mathcal{P} is recovered from the mixed-state analog of the Dyson series, $\mathcal{P} = \sum_{n=0}^{\infty} \mathcal{P}^{(n)}$, to add back individual photon-counting events to the dynamics. The perturbations $\mathcal{P}^{(n)}$ are source propagators conditioned on detecting n photons between the initial time t_0 and the final time t , and they can be solved recursively by $\mathcal{P}^{(n)}(t, t_0) = \int_{t_0}^t \mathcal{P}^{(0)}(t, t')\mathcal{J}(t')\mathcal{P}^{(n-1)}(t', t_0)dt'$ [23]. From this perspective, each photon-counting event adds a jump \mathcal{J} at some time t' . The result is then given by integrating over all possible jump times t' between t_0 and t .

This photon-number decomposition (see Fig. 1c) provides the state of the source $\hat{\rho}^{(n)}(t) = \mathcal{P}^{(n)}(t, t_0)\hat{\rho}(t_0)$ given that n photons have been detected between time t_0 and t , which occurs with the probability of $p^{(n)}(t) = \text{Tr}[\hat{\rho}^{(n)}(t)]$. The recursive solution, which can be evaluated using the scattering module in the QuTiP Python package [29], implies that simulating n th-order time-integrated quantities requires solving an n -dimensional time integral. Hence, the time to compute $p^{(n)}$ scales exponentially, roughly following $\mathcal{O}(N_{dt}^n)$ where N_{dt} is the number of time steps needed to resolve the time dynamics.

To avoid this unfavorable scaling, one can exploit the relationship between the detector efficiency and the ZPG. If a photon is detected with probability η , the ZPG becomes $\mathcal{L}_{\eta}^{(0)} = \mathcal{L} - \eta\mathcal{J}$. At the level of probabilities, $p_{\eta}^{(0)}$ now depends on η and can be written as a linear combination of all lossless $p^{(n)}$ weighted by powers of the loss coefficient $1 - \eta$. That is, one can obtain the loss relation, or probability generating function, $p_{\eta}^{(0)} = \sum_{n=0}^{\infty} (1 - \eta)^n p^{(n)}$ that is known in linear optics [24, 25, 30], but now connected directly to the source dynamics through the solution to the ZPG.

Assuming the pulse is finite, there is an N such that $p^{(n)} \simeq 0$ for $n > N$. By evaluating $p_{\eta}^{(0)}$ for N unique values of η along

with $p_0^{(0)} = 1$, all $p^{(n)}$ up to $n = N$ can be estimated by inverting the loss relation [24, 25]. Thus, all non-negligible $p^{(n)}$ are obtained by solving the ZPG just N times. When neglecting the inversion step, which for reasonable N is negligible compared to solving the dynamics, this leads to $\mathcal{O}(NN_t)$ scaling where N_t is the number of time steps needed to solve the master equation until t , which can be much smaller than N_{dt} .

The loss relation is a special case of a general relation that extends to the conditional states $\hat{\rho}^{(n)}$ and propagators $\mathcal{P}^{(n)}$ for any complex η . In fact, the solution to the effective master equation defined by a ZPG is equivalent to the \mathcal{Z} -transform of the set of conditional propagators: $\mathcal{Z}\{\mathcal{P}^{(n)}\} = \mathcal{G}_z$ where $\mathcal{Z}\{\mathcal{P}^{(n)}\} \equiv \sum_{n=0}^{\infty} \mathcal{P}^{(n)}z^{-n}$. The generating maps \mathcal{G}_z are given by $\mathcal{G}_z(t, t_0) = \mathcal{T} \exp[\int_{t_0}^t \mathcal{L}_z^{(0)}(t')dt']$ where $\mathcal{L}_z^{(0)} = \mathcal{L} - (1 - z^{-1})\mathcal{J}$ for $z \in \mathbb{C}$. Thus, the decomposition is obtained by the inverse transform $\mathcal{P}^{(n)} = \mathcal{Z}^{-1}\{\mathcal{G}_z\}$ for a set of unique z .

A proof of this is given in the supplementary [31] by taking the n th derivative of \mathcal{G}_z with respect to z^{-1} and then showing that $z \rightarrow \infty$ provides the lossless propagator $\mathcal{P}^{(n)}$. It follows from linearity that $\mathcal{G}_z\hat{\rho}(t_0) = \sum_{n=0}^{\infty} \hat{\rho}^{(n)}z^{-n}$ and $\text{Tr}[\mathcal{G}_z\hat{\rho}(t_0)] = \sum_{n=0}^{\infty} p^{(n)}z^{-n}$. The loss relation is recovered from the latter expression when $z = (1 - \eta)^{-1}$. However, instead of inverting a loss relation which can suffer from numerical instability, the set of $\{z\}$ can now be chosen such that $z^N = 1$. Then, \mathcal{Z} becomes a discrete Fourier transform and \mathcal{Z}^{-1} can be implemented using a fast Fourier transform (FFT) algorithm [32].

Consider the textbook example of a two-level emitter driven by a square pulse (see Fig. 2a), for which there is an analytic solution for $p^{(n)}$ [22]. To best illustrate the method, I choose a pulse with an integrated area of $\Theta = 10\pi$ and a temporal width $\tau = 2\gamma^{-1}$ of twice the emitter lifetime γ^{-1} , so that the distribution is both non-classical and non-negligible up to $p^{(6)}$ (see Fig. 2b). The QuTiP package in Python can then be used to solve the ZPG and the photon number probabilities are reconstructed using an FFT (see code availability). Figure 2c shows that the simulated probability distribution quickly converges to the exact solution when increasing the truncation N such that the relative error is $< 10^{-12}$ for $p^{(n)}$ up to $n = 6$ for $N = 14$. In addition, Figure 2d shows an exponential speedup over the recursive integration method implemented using the QuTiP scattering module.

Multi-mode scenario.—It is straightforward to generalize the method to M modes each monitored by a detector [31]. In this case, the ZPG is $\mathcal{L}_z^{(0)} = \mathcal{L} - \eta(z)\mathcal{J}$, where $\mathcal{J} = (\mathcal{J}_1, \dots, \mathcal{J}_M)$ is a vector of linear superoperators \mathcal{J}_j describing the action induced on the source by detecting a photon at the j th detector, and $\eta = (\eta_1, \dots, \eta_M)$ is a vector of corresponding detector efficiencies $\eta_j = 1 - z_j^{-1}$ for $z_j \in \mathbb{C}$. Then, applying \mathcal{Z} gives

$$\mathcal{T} \exp\left[\int_{t_0}^t \mathcal{L}_z^{(0)}(t')dt'\right] = \sum_{\mathbf{n}} \mathcal{P}^{(\mathbf{n})}(t, t_0) \prod_{j=1}^M z_j^{-n_j}, \quad (1)$$

where $\mathbf{n} = (n_1, \dots, n_M)$ is the vector of detected photon numbers and $\mathcal{P}^{(\mathbf{n})}$ is the propagator conditioned on observing \mathbf{n} .

To elaborate, consider a system of M independent sources each evolving with dynamics governed by a Lindbladian \mathcal{L}_i

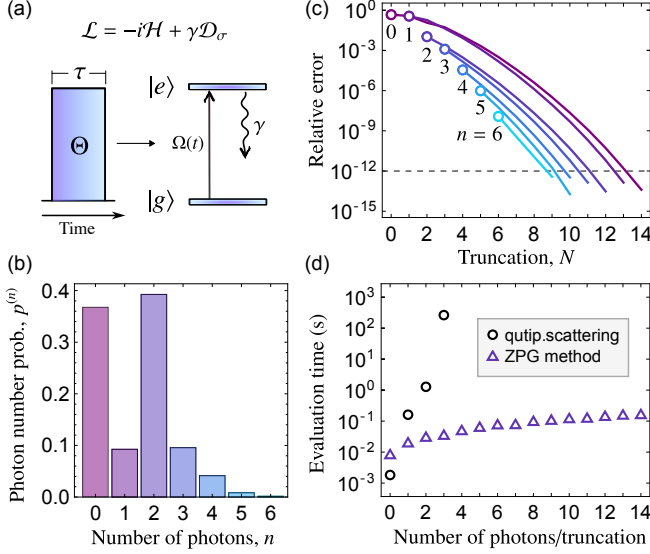


FIG. 2. **Scattering photons off a two-level emitter.** (a) A square pulse with temporal width τ and area Θ driving a two-level emitter with decay rate γ , whose evolution is governed by the Lindbladian $\mathcal{L} = -i\mathcal{H} + \gamma\mathcal{D}_\sigma$, where $\mathcal{H}\hat{\rho} = \Omega(t)[\hat{\sigma} + \hat{\sigma}^\dagger, \hat{\rho}]/2$, $\hat{\sigma} = |g\rangle\langle e|$, and $\mathcal{D}_\sigma\hat{\rho} = \hat{\sigma}\hat{\rho}\hat{\sigma}^\dagger - \{\hat{\sigma}^\dagger\hat{\sigma}, \hat{\rho}\}/2$. The zero-photon generator (ZPG) is then $\mathcal{L}_z^{(0)} = \mathcal{L} - \eta(z)\mathcal{J}$, where $\mathcal{J}\hat{\rho} = \gamma\hat{\sigma}\hat{\rho}\hat{\sigma}^\dagger$ and $\eta(z) = 1 - z^{-1}$. (b) Exact photon number probabilities $p^{(n)}$ for $\tau = 2\gamma^{-1}$ and $\Theta = 10\pi$ using analytic integration. (c) Convergence of the simulated distribution to the exact solution with increasing truncation N of ZPG sampling points. (d) Numerical simulation time using the QuTiP scattering module (black circles) for 2 significant digits of precision compared to the ZPG method (purple triangles) with up to 12 significant digits.

(see Fig. 3a). Each source satisfies an input-output relation $\hat{a}_i = \sqrt{\gamma_i}\hat{c}_i + \hat{a}_{i,\text{in}}$ arising from a linear dipole interaction in the Markovian limit [28], where \hat{a}_i is the mode collecting emission, and \hat{c}_i is the system operator coupled to the electromagnetic continuum with rate γ_i . The operator $\hat{a}_{i,\text{in}}$ describes the quantum fluctuations of the electromagnetic vacuum input to the i th source, which are inconsequential when simulating photon-counting measurements for independently driven sources [20]. Also suppose there is a linear-optical unitary transformation \hat{U} on the collection modes producing output modes $\hat{d}_j = \sum_i U_{ji}\hat{a}_i$ that are each monitored by a detector.

By choosing to decompose the dynamics using \mathcal{J}_j that describe the detection of a photon at the j th detector after the unitary transformation, the ZPG can be written as

$$\mathcal{L}_z^{(0)} = \mathcal{L} - \mathcal{J}^+ \cdot \hat{\eta}'(z) \cdot \mathcal{J}^-, \quad (2)$$

where $\mathcal{L} = \sum_{i=0}^M \mathcal{L}_i$, and $\mathcal{J}^\pm = (\mathcal{J}_1^\pm, \dots, \mathcal{J}_M^\pm)$ with $\mathcal{J}_i^-\hat{\rho} = \sqrt{\gamma_i}\hat{c}_i\hat{\rho}$ and $\mathcal{J}_i^+\hat{\rho} = \sqrt{\gamma_i}\hat{\rho}\hat{c}_i^\dagger$. The matrix $\hat{\eta}'(z) = \hat{U}^\dagger\hat{\eta}(z)\hat{U}$ is the unitary transformation of the diagonal matrix $\hat{\eta}(z)$ of virtual efficiencies $\eta(z)$. Note that a source k can also produce uncorrelated vacuum by setting $\gamma_k = 0$ and neglecting \mathcal{L}_k .

The multi-mode ZPG strongly resembles a Hamiltonian of a coupled many-body system. By expanding the coupling term, it is apparent that each source experiences a local shift $\mathcal{L}_i - \eta'_{ii}\mathcal{J}_i^+\mathcal{J}_i^-$ and there is a two-body conditional coupling

$\eta'_{ij}\mathcal{J}_i^+\mathcal{J}_j^- + \eta'_{ji}\mathcal{J}_i^-\mathcal{J}_j^+$ between sources that depends critically on both $\hat{\eta}$ and \hat{U} . For example, if $\hat{\eta}$ commutes with \hat{U} , then the coupling vanishes. If $\hat{\eta}$ is the identity, then the observation of no photons implies each input was vacuum, and hence all sources must follow their local zero-photon evolution. If $\hat{\eta}$ is zero, then the measurement provides no information and each source independently evolves following \mathcal{L}_i .

Consider again a two-level emitter driven by a square pulse, but now with $\Theta = \pi$ so that the emission converges to an ideal single photon in the limit $\tau \rightarrow 0$. To demonstrate the ZPG method for multi-mode simulations, I compute the total variation distance (TVD) averaged over 10 Haar random 4×4 unitary matrices for the simulated probability distribution relative to the exact distribution computed using Perceval [33] (see code availability). Figure 3c shows that the TVD approaches 0 as the pulse width decreases, verifying that the ZPG method captures all correlations due to quantum interference.

The time to simulate the full distribution for M two-level emitters and M detectors increases exponentially (see Fig. 3d), as expected due to the increasing Hilbert space size and number of outcomes. However, the speedup provided by the ZPG method allows to simulate the exact time-integrated quantum dynamics, interference, and full photon-number resolved probability distribution of pulsed emission from up to six emitters in less than 3 hours on a laptop using Python. Preliminary work also suggests that optimization using Julia (see code availability) or C++ could decrease simulation time by up to two orders of magnitude.

Discussion.— The ZPG method has multiple extensions and applications. Notably, the ZPG can be evaluated independently for each configuration z , allowing for embarrassingly parallel computation. The set of z and corresponding \mathcal{Z} -transform can also be designed to efficiently provide other quantities that can be written as a function of $p^{(n)}$. For example, it can provide threshold detection probabilities directly [30, 31], which drastically reduces simulation times (see Fig. 3d) and is relevant for state-of-the-art photonic devices [34]. Threshold detection can also be used to derive efficient algorithms to simulate figures of merit for single-photon sources such as brightness, single-photon purity, and indistinguishability [31]. In addition, the method can simulate integrated Wigner functions at individual points in phase space [35] by displacing the light with a local oscillator and setting $z = -1$ so that \mathcal{Z} becomes the parity summation.

The method is fully compatible with the SLH framework for quantum cascaded networks [36], which allows to simulate sources with non-vacuum input fields [37] or circuits containing non-linear materials. The unitary property of \hat{U} can also be relaxed to take into account non-uniform losses. Simulated measurements can involve many different degrees of freedom of light emitted by one or more sources, such as polarization, frequency, spatial mode, and time bin. Degrees of freedom can be binned together to accurately represent experimental setups while drastically reducing simulation time [32]. Moreover, since the method gives the dynamics conditioned

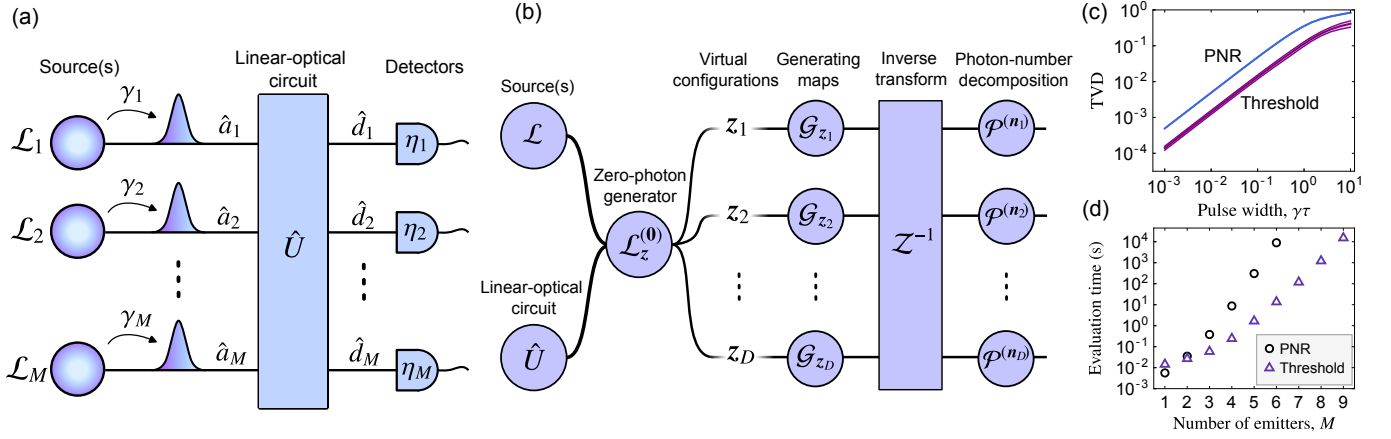


FIG. 3. **Multi-mode photon-number decomposition.** (a) An ensemble of sources, each described by a Lindbladian \mathcal{L}_i , spontaneously emit pulses into their respective collection modes \hat{a}_i at the rate γ_i . These pulses enter into a linear-optical circuit described by a unitary matrix \hat{U} . Each output mode \hat{d}_i is monitored by a detector with an efficiency η_i . (b) The absence of detection at the output of the circuit conditions the sources to evolve following the zero-photon generator (ZPG) $\mathcal{L}_z^{(0)} = \mathcal{L} - \boldsymbol{\eta}(\mathbf{z}) \cdot \mathcal{J}$, where $\mathcal{L} = \sum_{i=1}^M \mathcal{L}_i$ is the total Lindbladian, $\boldsymbol{\eta}$ is the vector of complex detector efficiencies and \mathcal{J} is the vector of linear superoperators acting on the sources when detecting photons at the output of the circuit. The ZPG is solved D times for unique virtual configurations \mathbf{z} , where D is the number of photon-detection outcomes \mathbf{n} with non-negligible probability $p^{(n)}$. Applying the inverse transform \mathcal{Z}^{-1} to the set of D generating maps $\{\mathcal{G}_{\mathbf{z}_i}\}$, generating states $\{\mathcal{G}_{\mathbf{z}_i}\hat{\rho}(t_0)\}$, or generating probabilities $\{\text{Tr}[\mathcal{G}_{\mathbf{z}_i}\hat{\rho}(t_0)]\}$ provides the set of conditional propagators $\{\mathcal{P}^{(n)}\}$, conditional states $\{\hat{\rho}^{(n)}\}$, or probabilities $\{p^{(n)}\}$, respectively. (c) Average total variation distance (TVD) over 10 Haar-random \hat{U} relative to perfect single-photon interference for emission from $M = 4$ identical two-level emitters each driven by square pulses with area $\Theta = \pi$ and a varying pulse width τ . The TVD for simulated photon-number resolved (PNR) and threshold detection distributions both converge to their respective exact distributions computed using the Perceval package in Python as $\tau \rightarrow 0$. The standard deviation of the TVD is shown by the thickness of each curve. (d) The time needed to simulate a full PNR or threshold detection distribution in Python as a function of the number of two-level emitters producing single photons.

on photon-counting measurements, it can be used to simulate realistic conditional quantum channels for spin-photon entanglement [38] and photon-heralded spin-spin entanglement protocols for quantum communication [23, 39, 40].

Conclusion.—By exploiting the relationship between conditional evolution and a set of virtual detector configurations, it is possible to circumvent multi-variable integration when simulating time-integrated photon counting for sources following Markovian dynamics. This provides a significant computational speedup for simulating photon-counting experiments using time-dynamic quantum systems, which has a broad range of applications for developing quantum photonic technology. Further studies could extend the concept of a ZPG to non-Markovian dynamics, linear-optical circuits that include delay lines, and measurement feed-forward.

The ZPG defines an equation of motion sufficient to simulate a photonic quantum computation. It is promising to develop an analogy with the Hamiltonian dynamics of many-qubit systems to uncover algorithms that exploit noise to solve the ZPG efficiently, such as tensor network techniques [41, 42]. The coupling between sources during the photonic measurement, and hence the amount of entanglement, depends on the efficiency, unitary transformation, and coherence between emission from each source. Thus the ZPG also has features in line with classical simulability of boson sampling problems [43–45], which provides a new perspective that could lead to further studies on the complexity and quantum advantage for photonic quantum information processing.

Acknowledgements.—This work was supported by the European Innovation Council (EIC) Accelerator program through the Scalable Entangled-Photon based Optical Quantum Computers (SEPOQC) grant. I would like to thank Paul Hilaire for reading the manuscript and providing feedback; Shane Mansfield, Rawad Mezher, and Emilio Annoni for discussions about theory; Fabien Thollot for help with clarification of concepts; Sharon David and Albert Adiyatullin for testing implementations; and Jean Senellart, Nicolas Heurtel, Timothée Goubault de Brugière, Raksha Singla, Valentin Guichard, Hubert Lam, Nadia Belabas, Pascale Senellart, and H  l  ne Olivier for thought-provoking questions and comments.

Code availability.—All the code used to produce the numerical results will be made available upon publication.

* stephen.wein@quandela.com

- [1] F. Flamini, N. Spagnolo, and F. Sciarrino, Reports on Progress in Physics **82**, 016001 (2018).
- [2] S. Pirandola, B. R. Bardhan, T. Gehring, C. Weedbrook, and S. Lloyd, Nature Photonics **12**, 724 (2018).
- [3] H. J. Kimble, Nature **453**, 1023 (2008).
- [4] C. Simon, Nature Photonics **11**, 678 (2017).
- [5] S. Wehner, D. Elkouss, and R. Hanson, Science **362**, eaam9288 (2018).
- [6] E. Knill, R. Laflamme, and G. J. Milburn, Nature **409**, 46 (2001).

- [7] P. Kok, W. J. Munro, K. Nemoto, T. C. Ralph, J. P. Dowling, and G. J. Milburn, *Reviews of Modern Physics* **79**, 135 (2007).
- [8] S. Bartolucci, P. Birchall, H. Bombin, H. Cable, C. Dawson, M. Gimeno-Segovia, E. Johnston, K. Kieling, N. Nickerson, M. Pant, *et al.*, *Nature Communications* **14**, 912 (2023).
- [9] J. L. O'Brien, A. Furusawa, and J. Vučković, *Nature Photonics* **3**, 687 (2009).
- [10] C. Couteau, *Contemporary Physics* **59**, 291 (2018).
- [11] I. Aharonovich, D. Englund, and M. Toth, *Nature Photonics* **10**, 631 (2016).
- [12] N. H. Lindner and T. Rudolph, *Physical Review Letters* **103**, 113602 (2009).
- [13] H. P. Specht, C. Nölleke, A. Reiserer, M. Uphoff, E. Figueroa, S. Ritter, and G. Rempe, *Nature* **473**, 190 (2011).
- [14] R. Loudon, *The quantum theory of light* (OUP Oxford, 2000).
- [15] C.-K. Hong, Z.-Y. Ou, and L. Mandel, *Physical Review Letters* **59**, 2044 (1987).
- [16] A. Kiraz, M. Atatüre, and A. Imamoglu, *Physical Review A* **69**, 032305 (2004).
- [17] The QuTiP Python package for quantum dynamics does not have built-in functionality for solving integrated field correlations for more than two detectors. Multi-photon probabilities can be computed using the scattering module, but this relies on recursive integration that is practical only for a few photons.
- [18] T. Grange, G. Hornecker, D. Hunger, J.-P. Poizat, J.-M. Gérard, P. Senellart, and A. Auffèves, *Physical Review Letters* **114**, 193601 (2015).
- [19] S. Wein, N. Lauk, R. Ghobadi, and C. Simon, *Physical Review B* **97**, 205418 (2018).
- [20] H. Carmichael, *An open systems approach to quantum optics: lectures presented at the Université Libre de Bruxelles, October 28 to November 4, 1991*, Vol. 18 (Springer Science & Business Media, 2009).
- [21] K. A. Fischer, R. Trivedi, and D. Lukin, *Physical Review A* **98**, 023853 (2018).
- [22] K. A. Fischer, R. Trivedi, V. Ramasesh, I. Siddiqi, and J. Vučković, *Quantum* **2**, 69 (2018).
- [23] S. C. Wein, J.-W. Ji, Y.-F. Wu, F. K. Asadi, R. Ghobadi, and C. Simon, *Physical Review A* **102**, 033701 (2020).
- [24] A. R. Rossi, S. Olivares, and M. G. Paris, *Physical Review A* **70**, 055801 (2004).
- [25] G. Zambra, A. Andreoni, M. Bondani, M. Gramegna, M. Genovese, G. Brida, A. Rossi, and M. G. Paris, *Physical Review Letters* **95**, 063602 (2005).
- [26] I notate superoperators with a calligraphic font and operators using a hat. All superoperators act on everything to their right.
- [27] D. Manzano, *Aip Advances* **10**, 025106 (2020).
- [28] C. W. Gardiner and M. J. Collett, *Physical Review A* **31**, 3761 (1985).
- [29] J. R. Johansson, P. D. Nation, and F. Nori, *Computer Physics Communications* **183**, 1760 (2012).
- [30] J. F. Bulmer, S. Paesani, R. S. Chadwick, and N. Quesada, *arXiv preprint arXiv:2202.04600* (2022).
- [31] See supplemental material.
- [32] B. Seron, L. Novo, A. Arkhipov, and N. J. Cerf, *arXiv preprint arXiv:2212.09643* (2022).
- [33] N. Heurtel, A. Fyrrillas, G. de Glinasty, R. Le Bihan, S. Malherbe, M. Pailhas, E. Bertasi, B. Bourdoncle, P.-E. Emeriau, R. Mezher, *et al.*, *Quantum* **7**, 931 (2023).
- [34] N. Maring, A. Fyrrillas, M. Pont, E. Ivanov, P. Stepanov, N. Margaria, W. Hease, A. Pishchagin, T. H. Au, S. Boissier, *et al.*, *arXiv preprint arXiv:2306.00874* (2023).
- [35] K. Banaszek, C. Radzewicz, K. Wódkiewicz, and J. Kasiński, *Physical Review A* **60**, 674 (1999).
- [36] J. Combes, J. Kerckhoff, and M. Sarovar, *Advances in Physics: X* **2**, 784 (2017).
- [37] A. H. Kiilerich and K. Mølmer, *Physical Review Letters* **123**, 123604 (2019).
- [38] N. Coste, D. Fioretto, N. Belabas, S. Wein, P. Hilaire, R. Frantzeskakis, M. Gundin, B. Goes, N. Somaschi, M. Morassi, *et al.*, *arXiv preprint arXiv:2207.09881* (2022).
- [39] M. Atatüre, D. Englund, N. Vamivakas, S.-Y. Lee, and J. Wrachtrup, *Nature Reviews Materials* **3**, 38 (2018).
- [40] M. Pompili, S. L. Hermans, S. Baier, H. K. Beukers, P. C. Humphreys, R. N. Schouten, R. F. Vermeulen, M. J. Tiggeleman, L. dos Santos Martins, B. Dirkse, *et al.*, *Science* **372**, 259 (2021).
- [41] R. Orús, *Nature Reviews Physics* **1**, 538 (2019).
- [42] C. Oh, K. Noh, B. Fefferman, and L. Jiang, *Physical Review A* **104**, 022407 (2021).
- [43] A. E. Moylett, R. García-Patrón, J. J. Renema, and P. S. Turner, *Quantum Science and Technology* **5**, 015001 (2019).
- [44] R. García-Patrón, J. J. Renema, and V. Shchesnovich, *Quantum* **3**, 169 (2019).
- [45] R. Mezher and S. Mansfield, *arXiv preprint arXiv:2202.04735* (2022).

Supplemental material: Simulating time-integrated photon counting using a zero-photon generator

Stephen C. Wein

Quandela SAS, 10 Boulevard Thomas Gobert, 91120 Palaiseau, France

PHOTON-NUMBER DECOMPOSITION USING A Z-TRANSFORM

To demonstrate that the zero-photon conditional propagator $\mathcal{P}_\eta^{(0)}(t, t_0) = \mathcal{T} \exp[\int_{t_0}^t \mathcal{L}_\eta^{(0)}(t') dt']$ defined by the ZPG $\mathcal{L}_\eta^{(0)}(t) = \mathcal{L}(t) - \eta \mathcal{J}(t)$ is equal to the generating map $\mathcal{G}_z = \mathcal{Z}\{\mathcal{P}^{(n)}\} = \sum_{n=0}^{\infty} \mathcal{P}^{(n)} z^{-n}$ for $z = (1 - \eta)^{-1}$, we can equate each coefficient of the polynomial by showing that $d^n \mathcal{P}_\eta^{(0)} / dL^n|_{L \rightarrow 0} = n! \mathcal{P}^{(n)}$ where $L = 1 - \eta$ is a complex loss coefficient. Note we already have $\mathcal{P}_\eta^{(n)}|_{L \rightarrow 0} = \mathcal{P}^{(n)}$ for all n by definition and so it suffices to show that $d\mathcal{P}_\eta^{(n)} / dL = (n + 1) \mathcal{P}_\eta^{(n+1)}$ for all n .

To proceed we can first consider the case where \mathcal{L} and \mathcal{J} do not depend on time. Then $\mathcal{P}_\eta^{(0)}(t, t_0) = e^{(t-t_0)(\mathcal{L}-\eta\mathcal{J})}$. For the base case showing $n = 0$ implies $n = 1$, we can make use of the Wilcox formula for the exponential map:

$$\frac{d}{dx} e^{A(x)} = \int_0^1 e^{\alpha A(x)} \frac{dA(x)}{dx} e^{(1-\alpha)A(x)} d\alpha \quad (\text{S1})$$

to obtain

$$\frac{d}{dL} \mathcal{P}_\eta^{(0)}(t, t_0) = (t - t_0) \int_0^1 e^{\alpha(t-t_0)(\mathcal{L}-\eta\mathcal{J})} \mathcal{J} e^{(1-\alpha)(t-t_0)(\mathcal{L}-\eta\mathcal{J})} d\alpha \quad (\text{S2})$$

By substituting $\alpha(t - t_0) = t - t'$ we get

$$\begin{aligned} \frac{d}{dL} \mathcal{P}_\eta^{(0)}(t, t_0) &= \int_{t_0}^t e^{(t-t')(\mathcal{L}-\eta\mathcal{J})} \mathcal{J} e^{(t'-t_0)(\mathcal{L}-\eta\mathcal{J})} dt' \\ &= \int_{t_0}^t \mathcal{P}_\eta^{(0)}(t, t') \mathcal{J} \mathcal{P}_\eta^{(0)}(t', t_0) dt' \\ &= \mathcal{P}_\eta^{(1)}(t, t_0). \end{aligned} \quad (\text{S3})$$

Now, if we assume $d\mathcal{P}_\eta^{(n-1)} / dL = n \mathcal{P}_\eta^{(n)}$, then

$$\begin{aligned} \frac{d}{dL} \mathcal{P}_\eta^{(n)}(t, t_0) &= \frac{d}{dL} \int_{t_0}^t \mathcal{P}_\eta^{(0)}(t, t') \mathcal{J} \mathcal{P}_\eta^{(n-1)}(t', t_0) dt' \\ &= \int_{t_0}^t \frac{d\mathcal{P}_\eta^{(0)}(t, t')}{dL} \mathcal{J} \mathcal{P}_\eta^{(n-1)}(t', t_0) dt' + \int_{t_0}^t \mathcal{P}_\eta^{(0)}(t, t') \mathcal{J} \frac{d\mathcal{P}_\eta^{(n-1)}(t', t_0)}{dL} dt' \\ &= \int_{t_0}^t \mathcal{P}_\eta^{(1)}(t, t') \mathcal{J} \mathcal{P}_\eta^{(n-1)}(t', t_0) dt' + n \int_{t_0}^t \mathcal{P}_\eta^{(0)}(t, t') \mathcal{J} \mathcal{P}_\eta^{(n)}(t', t_0) dt' \\ &= (n + 1) \mathcal{P}_\eta^{(n+1)}(t, t_0). \end{aligned} \quad (\text{S4})$$

The last step combining the two terms makes use of the relation

$$\int_{t_0}^t \mathcal{P}_\eta^{(n)}(t, t') \mathcal{J} \mathcal{P}_\eta^{(k)}(t', t_0) dt' = \mathcal{P}_\eta^{(n+k+1)}(t, t_0), \quad (\text{S5})$$

a proof of which is in the appendix of Ref. [1].

To extend this to the time-dependent case, we can divide the total time interval into N piece-wise time-independent parts each of length $dt = (t - t_0)/N$, beginning at time t_{i-1} and ending at time t_i . Since each $\mathcal{G}_z(t_i, t_{i-1})$ satisfies an effective master equation, we simply have $\mathcal{G}_z(t, t_0) = \prod_{i=1}^N \mathcal{G}_z(t_i, t_{i-1})$. Then, we can substitute the time-independent solution and regroup terms based on the total number of photons

$$\begin{aligned} \mathcal{G}_z(t, t_0) &= \prod_{i=1}^N \sum_{n=0}^{\infty} \mathcal{P}^{(n)}(t_i, t_{i-1}) z^{-n} \\ &= \mathcal{P}^{(0)}(t, t_0) + z^{-1} \sum_{i=1}^N \mathcal{P}^{(0)}(t, t_i) \mathcal{P}^{(1)}(t_i, t_{i-1}) \mathcal{P}^{(0)}(t_{i-1}, t_0) + \dots, \end{aligned} \quad (\text{S6})$$

where $t_N = t$. Taking the limit $dt \rightarrow 0$, we can find that $\mathcal{P}^{(n)}(t_i, t_{i-1})$ for $n \geq 2$ are negligible compared to all combinations of n single-photon propagators $\mathcal{P}^{(1)}$ among bins of vacuum $\mathcal{P}^{(0)}$. In addition, \mathcal{J} becomes localized at $t_{i-1} \leq t' \leq t_i$. So, substituting the definition of $\mathcal{P}^{(1)}$ and moving to the continuum limit we get

$$\begin{aligned}
\mathcal{G}_z(t, t_0) &= \mathcal{P}^{(0)}(t, t_0) + z^{-1} \sum_{i=1}^N \int_{t_{i-1}}^{t_i} \mathcal{P}^{(0)}(t, t_i) \mathcal{P}^{(0)}(t_i, t') \mathcal{J}(t_i) \mathcal{P}^{(0)}(t', t_{i-1}) \mathcal{P}^{(0)}(t_{i-1}, t_0) dt' + \dots \\
&= \mathcal{P}^{(0)}(t, t_0) + z^{-1} \sum_{i=1}^N \int_{t_{i-1}}^{t_i} \mathcal{P}^{(0)}(t, t') \mathcal{J}(t_i) \mathcal{P}^{(0)}(t', t_0) dt' + \dots \\
&= \mathcal{P}^{(0)}(t, t_0) + z^{-1} \int_{t_0}^t \mathcal{P}^{(0)}(t, t') \mathcal{J}(t') \mathcal{P}^{(0)}(t', t_0) dt' + \dots \\
&= \sum_{n=0}^{\infty} \mathcal{P}^{(n)}(t, t_0) z^{-n}.
\end{aligned} \tag{S7}$$

Although I only illustrated the regrouping for the $n = 1$ terms, the same argument applies to the regrouping of the $n \geq 2$ terms.

Multimode scenario

The photon-number decomposition has a straightforward extension to the multi-mode scenario [2]. The perturbative series becomes $\mathcal{P} = \sum_n \mathcal{P}^{(n)}$ where

$$\mathcal{P}^{(n+\mathbf{e}_i)}(t, t_0) = \int_{t_0}^t \mathcal{P}^{(0)}(t, t') \mathcal{J}_i(t') \mathcal{P}^{(n)}(t', t_0) dt', \tag{S8}$$

where \mathbf{e}_i is the i th unit vector. The zero-photon propagator $\mathcal{P}^{(0)}(t, t_0)$ is the solution to the effective master equation $d\hat{\rho}^{(0)}(t)/dt = \mathcal{L}^{(0)}(t)\hat{\rho}^{(0)}(t)$ where the ZPG is

$$\mathcal{L}^{(0)}(t) = \mathcal{L}(t) - \sum_i \mathcal{J}_i(t). \tag{S9}$$

Multiplying a detector efficiency η_i to each \mathcal{J}_i , the ZPG takes the form given in the main text. Since adding additional detectors only adds independent perturbations linearly to the ZPG, the proof of the single-mode scenario immediately extends due to the linearity of the derivative in the Wilcox formula.

THRESHOLD DETECTION DECOMPOSITION

Often measurements are performed where a detector ‘clicks’ if it receives one or more photons. We denote probability of that the detector clicks as the brightness $\beta = \sum_{n=1}^{\infty} p^{(n)} = 1 - p^{(0)}$, where $p^{(0)}$ is the probability that the detector does not click. The conditional state associated with the threshold detection probability is then similarly given by the complement of the zero-photon conditional state: the bright conditional state $\hat{\beta} = \hat{\rho} - \hat{\rho}^{(0)}$. Even more generally, the associated bright propagation superoperator is $\mathcal{B} = \mathcal{P} - \mathcal{P}^{(0)}$ [3]. In summary, we have $\beta(t) = \text{Tr}[\hat{\beta}(t)] = \text{Tr}[\mathcal{B}(t, t_0)\hat{\rho}(t_0)]$ for initial state $\hat{\rho}(t_0)$ of the system.

When there are multiple detectors, the threshold detection probabilities are more conveniently notated by $\beta^{(\mathbf{m})}$. Here, \mathbf{m} is a vector of binary numbers where 1 represents a threshold detection as opposed to \mathbf{n} in $p^{(\mathbf{n})}$, which represents the vector of detected photon numbers. It is important to note that, unlike the single-mode case, the threshold detection probability distribution $\beta^{(\mathbf{m})}$ cannot be computed by $1 - p^{(0)}$.

To recover the associated bright propagation superoperators $\mathcal{B}^{(\mathbf{m})}$ conditioned on the threshold detection outcome \mathbf{m} from the ZPG, we can notice that there is a special case of the transform where each z_i either tends to infinity (efficient limit, $L \rightarrow 0$) or tends to 1 (lossy limit, $L \rightarrow 1$). Then, $\prod_i z_i^{-n_i} \rightarrow \prod_i L_i^{n_i}$, where $L_i^{n_i}$ is either 1 or 0 (and $L_i^0 \rightarrow 1$ for $L_i \rightarrow 0$). We can then see that $L_i^{n_i} = L_i$ if $n_i \geq 1$ and $L_i^{n_i} = 1$ if $n_i = 0$. Hence, all terms $\mathcal{P}^{(\mathbf{n})} \prod_i L_i^{n_i}$ that differ by some $n_i \neq 0$ will be identical and sum to the associated $\mathcal{B}^{(\mathbf{n})} \prod_i L_i^{n_i}$. In this particular case, the transformation can be inverted [4] to obtain a solution for the threshold detection decomposition

$$\mathcal{B}^{(\mathbf{m})} = \sum_{\mathbf{z}} \mathcal{G}_{\mathbf{z}} \prod_i (-1)^{m_i + L_i} (1 - L_i)^{1 - m_i}, \tag{S10}$$

where $z_i = L_i^{-1}$ and $L_i = 1 - \eta_i$.

FIGURES OF MERIT FOR SINGLE-PHOTON SOURCES

An important figure of merit for single-photon sources is the integrated intensity auto-correlation defined by

$$g^{(2)} \equiv \frac{1}{\mu^2} \iint \langle \hat{a}^\dagger(t_1) \hat{a}^\dagger(t_2) \hat{a}(t_2) \hat{a}(t_1) \rangle dt_1 dt_2, \quad (\text{S11})$$

where $\mu = \int \langle \hat{a}^\dagger(t) \hat{a}(t) \rangle dt$ and \hat{a} is the photon annihilation operator of the waveguide collecting emission from the source. This expression is usually evaluated using an input-output relation to connect \hat{a} to a source operator, and then using quantum regression theorem to evaluate the corresponding two-time correlation function. In the QuTiP package [5], this can be accomplished using the `correlation_3op_2t()` function, but this requires solving the master equation over a two-dimensional space of detection times, which is inefficient if we only require the integrated result.

Knowing the photon-number probabilities $p^{(n)}$ from using a ZPG, we could instead reconstruct the second-order intensity auto-correlation of the pulsed light using the formula $g^{(2)} = \mu^{-2} \sum_n n(n-1)p^{(n)}$, where $\mu = \sum_n np^{(n)}$ is the average photon number. If there are many photons in the pulse, this formula is also not the most efficient way to compute $g^{(2)}$. Instead, we can use the concept of threshold detection to derive a new formula that estimates the integrated intensity correlation directly from zero-photon detection probabilities.

We can begin by recognizing that detection statistics converge to intensity correlations in the lossy regime [6]. To see why this is the case also for integrated measurements of pulses, consider the average detected photon number. A linear loss model implies that $\mu(\eta'\eta) = \eta'\mu(\eta)$ for some real and artificial efficiency η and η' , respectively. Provided that η' is small enough, we must have that μ converges to $p^{(1)}$. Similarly, if η' is small enough, we also have that $\beta^{(1)}$ converges to $p^{(1)}$. These observations immediately imply that the following formula can be used to evaluate μ from a single zero-photon probability

$$\mu(\eta) = \lim_{\eta' \rightarrow 0} \frac{1 - p_{\eta'\eta}^{(0)}}{\eta'}. \quad (\text{S12})$$

In practice, η' can be chosen small enough so that $p^{(n)} \ll p^{(1)}$ for $n > 1$.

This idea can be extended to $g^{(2)}$. In this case, we can imagine that we have a balanced Hanbury Brown-Twiss (HBT) setup described by the ZPG $\mathcal{L}_\eta^{(0)} = \mathcal{L} - \eta_1 \mathcal{J}_1 - \eta_2 \mathcal{J}_2$. Following Eq. (S10), and assuming $\mathcal{J}_1 = \mathcal{J}_2 = \eta \mathcal{J}$ for some additional efficiency parameter η , we have $\beta^{(1,1)}(\eta) = 1 - 2p_{\eta/2}^{(0)} + p_\eta^{(0)}$, where $p_\eta^{(0)} = \text{Tr}[\hat{\rho}_\eta^{(0)}]$ is evaluated from the single-mode ZPG $\mathcal{L}_\eta^{(0)} = \mathcal{L} - \eta \mathcal{J}$.

In the limit η is small, we have $g^{(2)} = 2p^{(2)}/\mu^2$, $\mu = 1 - p^{(0)}$ and also $p^{(2)} = 2\beta^{(1,1)}$. Thus, $g^{(2)}$ can be estimated using the formula

$$g^{(2)} = \frac{4}{\mu^2} \lim_{\eta \rightarrow 0} \frac{1 - 2p_{\eta/2}^{(0)} + p_\eta^{(0)}}{\eta^2}. \quad (\text{S13})$$

Note that, unlike μ , $g^{(2)}$ is a loss-independent quantity. since we can estimate μ from either $p_\eta^{(0)}$ or $p_{\eta/2}^{(0)}$, this implies that it is possible to estimate $g^{(2)}$ by solving for just two final states of the effective master equation, which can provide orders of magnitude improvement in computational time compared to taking a time integral over the two-time intensity correlation.

The above approach can be extended to compute the m th order intensity auto-correlations $g^{(m)}$, which we do not present here. However, for increasing order m , it becomes more difficult to achieve a high precision estimate due to needing a very small η^m to correctly normalize the result.

Furthermore, the indistinguishability is determined by measuring coincidence counts after Hong-Ou-Mandel (HOM) interference of two photons at a beam splitter. Thus, we can also apply the formula for $g^{(2)}$ in the case that the inputs to the beam splitter come from independent, but identical, sources. This provides a fast way to simulate indistinguishability [7] as well as other figures of merit determined from HOM interference such as the first- [8, 9] and second-order number coherence [10]. The downside compared to the standard approach of computing the two-time amplitude correlation [7] is that the ZPG method requires simulating the evolution of two sources rather than one. The ZPG method still seems to provide a speedup in most cases, access to multiple figures of merit simultaneously, and can account for the interference of emitters with different properties. However, it can be slower than the standard approach if the Hilbert space of a single source is quite large and if only the indistinguishability of photons from a single source is needed. A possible way around this problem would be to derive a ZPG from a time-delay master equation that explicitly accounts for the delay line in a HOM experiment, so that one source can be simulated twice, but with feedback from the first simulation.

* stephen.wein@quandela.com

- [1] S. C. Wein, arXiv preprint arXiv:2105.06580 (2021).
- [2] S. C. Wein, J.-W. Ji, Y.-F. Wu, F. K. Asadi, R. Ghobadi, and C. Simon, *Physical Review A* **102**, 033701 (2020).
- [3] N. Coste, D. Fioretto, N. Belabas, S. Wein, P. Hilaire, R. Frantzeskakis, M. Gundin, B. Goes, N. Somaschi, M. Morassi, *et al.*, arXiv preprint arXiv:2207.09881 (2022).
- [4] J. F. Bulmer, S. Paesani, R. S. Chadwick, and N. Quesada, arXiv preprint arXiv:2202.04600 (2022).
- [5] J. R. Johansson, P. D. Nation, and F. Nori, *Computer Physics Communications* **183**, 1760 (2012).
- [6] M. B. Plenio and P. L. Knight, *Reviews of Modern Physics* **70**, 101 (1998).
- [7] A. Kiraz, M. Atatüre, and A. Imamoglu, *Physical Review A* **69**, 032305 (2004).
- [8] J. Loredó, C. Antón, B. Reznichenko, P. Hilaire, A. Harouri, C. Millet, H. Ollivier, N. Somaschi, L. De Santis, A. Lemaître, *et al.*, *Nature Photonics* **13**, 803 (2019).
- [9] I. Wenniger, S. Thomas, M. Maffei, S. Wein, M. Pont, A. Harouri, A. Lemaître, I. Sagnes, N. Somaschi, A. Auffèves, *et al.*, arXiv preprint arXiv:2202.01109 (2022).
- [10] S. C. Wein, J. C. Loredó, M. Maffei, P. Hilaire, A. Harouri, N. Somaschi, A. Lemaître, I. Sagnes, L. Lanco, O. Krebs, *et al.*, *Nature Photonics* **16**, 374 (2022).